CrystEngComm

RSC Publishing

COMMUNICATION

View Article Online
View Journal | View Issue

Large-scale synthesis of uniform Cu_2O nanocubes with tunable sizes by *in-situ* nucleation†

Cite this: *CrystEngComm*, 2013, **15**, 2363

Received 28th November 2012,
Accepted 19th January 2013

DOI: 10.1039/c3ce26932a

www.rsc.org/crystengcomm

I-Chun Chang,[a] Po-Chin Chen,[a] Min-Chiao Tsai,[a] Ting-Ting Chen,[a] Min-Han Yang,[a] Hsin-Tien Chiu[b] and Chi-Young Lee*[a]

Uniform Cu_2O nanocubes with various sizes were synthesized by reducing $Cu(OH)_2$ using ascorbic acid in the presence of various amounts of sodium citrate. The monodispersed nanocubes with an edge length of approximately 80 nm used as an anode exhibit excellent lithium storage behavior.

Cuprous oxide (Cu_2O), an important p-type semiconductor with a direct band gap of ~2.00 eV,[1] is favored for its abundance, low cost, environmental friendliness and safety. It has been studied with a view to various applications including sensing,[2–4] photocatalysis,[5] use in Li-ion batteries,[6] CO oxidation,[7,8] and hydrogen production.[9] Recently, not only the size but also the shape of inorganic materials has been found strongly to affect their physical and chemical properties. The shape-controlling synthesis of Cu_2O micro or nanostructures has been successful. Various Cu_2O structures, such as cubes,[10] octahedra,[11] hollow structures[12,13] and nanowires,[14] have been synthesized *via* wet-chemical reduction. However, controlling the size of Cu_2O structures is more difficult than controlling their shape. Cu_2O tends to grow with a poor size distribution in a hydrophilic system. Huang *et al.*[10] synthesized Cu_2O nanocubes with various sizes by reducing $Cu(OH)_4^{2-}$ using sodium ascorbate in the presence of sodium dodecyl sulfate (SDS) as a capping agent. This seed-mediated method enables the sizes and shapes of nanocubes to be well-controlled. Unfortunately, the yield of this method is far from industrially acceptable.

This work develops a facile one-step nucleation-controlled method for synthesizing uniform sized tunable cubic crystalline Cu_2O with an excellent 87.5% yield (75 mg per batch). Generally, Cu_2O were fabricated by the reduction of $Cu(OH)_2$ or $Cu(OH)_4^{2-}$ species. Pre-capping of Cu^{2+} markedly reduces $Cu(OH)_2$ in the initial stage, resulting in a small amount of Cu_2O seeds which leads to the growth of larger sized Cu_2O nanocubes. Sodium citrate, a chelating agent for Cu^{2+}, was employed to the reaction solution prior to NaOH addition, the Cu^{2+} ions were chelated by citrate ions to form copper-citrate, which retards the precipitation of $Cu(OH)_2$ during the addition of NaOH. Increasing the amount of sodium citrate in the reaction solution yielded larger Cu_2O nanocubes. Furthermore, the performance of the submicron Cu_2O nanocube electrodes in Li-ion batteries was investigated.

Uniform Cu_2O nanocubes with various sizes were synthesized *via* a simple aqueous-based wet-chemical reduction process using citrate as a chelating agent. Table 1 presents the synthetic conditions and the properties of these Cu_2O nanocube samples. Fig. 1 shows the field-emission scanning electron microscopic (SEM) images of three nanocubes in this study. The size of the nanocubes increased with the sodium citrate concentration. As shown in Fig. 1a–c, each sample comprised a large amount of well-defined nanocubes. These nanocubes with high uniformity and monodispersion were perfectly cubic with {100} facets without any truncation. The lengths of the edges of nanocubes A, B and C were in the ranges 50–55, 65–70, and 75–80 nm, respectively. Control samples were also made in the absence of citrate or NaOH. In control sample 1, made without citrate in the reaction solution, aggregated small nanocubes with a large distribution of edge lengths in the range 35–45 nm were fabricated, as shown in Fig. S1, ESI.† In control sample 2, the reaction solution contained sodium citrate but not NaOH, and no precipitation occurred. This result demonstrates that nanocubes were formed only by the reduction of ascorbic acid in a basic solution.

An energy dispersive spectrum (EDS, Fig. S2, ESI†) reveals that the powder comprised Cu and O in a molar ratio of 2 : 1. The carbon signal was associated with the conductive carbon tape that was used to fix the sample to the SEM holder. The quantities of the obtained powders were related only to the amount of Cu^{2+} ions in solution and were approximately 75 mg for all samples, independently of the amount of trisodium citrate dehydrate that was used.

The crystallographic structure and phase purity of nanocube samples were examined by X-ray powder diffraction (XRD) and transmission electron microscopic (TEM) characterization. The intensities and positions of all reflection peaks were consistent

[a]*Department of Materials Science and Engineering, National Tsing Hua University Hsinchu, Taiwan 30043, R. O. C.. E-mail: cylee@mx.nthu.edu.tw*
[b]*Department of Applied Chemistry, National Chiao Tung University Hsinchu, Taiwan 30050, R. O. C.. E-mail: htchiu@faculty.nctu.edu.tw*

† Electronic supplementary information (ESI) available: SEM, EDS, CV, Galvanostatic charge–discharge curves. See DOI: 10.1039/c3ce26932a

Table 1 Molar ratio of copper sulfate : trisodium citrate dihydrate : sodium hydroxide and size distribution of Cu_2O nanocubes in samples A–C

Sample	$CuSO_4 : C_6H_5Na_3O_7{\cdot}2H_2O : NaOH$	Edge length (nm)	Yield (mg)	Estimated seed number (mM)	Estimated free Cu ion (mM)
Control 1	1 : 0.00 : 4	35–45	77.5	8.38×10^{-7}	3
A	1 : 0.25 : 4	50–55	74.0	3.53×10^{-7}	2.25
B	1 : 0.50 : 4	65–70	77.0	2.18×10^{-7}	1.50
C	1 : 0.75 : 4	75–80	76.9	1.14×10^{-7}	0.75
Control 2	1 : 0.75 : 0	N.A.	N.A.	N.A.	0.75

with those of cuprite Cu_2O (JCPDF No. 05-0667), as shown in Fig. S3, ESI.† Fig. 1d displays a low-magnification TEM image of powder C. It shows Cu_2O nanocubes with uniform shape with edge lengths of approximately 80 nm. Fig. 1e shows a single Cu_2O nanocube that is lying on its {100} face. Fig. 1f shows the corresponding selected area electron diffraction (SAED) pattern. The patterns reveal that the crystallographic zone axis is [001] and that the nanocubes are single crystals. These square diffraction patterns were indexed to the diffraction planes of cubic Cu_2O. The *d* spacing that was estimated from the spots closest to the center of the beam was 2.1 Å. This result is consistent with the *d* spacing between the Cu_2O (200) planes (JCPDF No. 05-0667). Fig. 1g presents high-resolution TEM images of a tilted Cu_2O nanocube, viewed along its <110> direction. Visible lattice fringes with *d*-spacings of ~3.04 Å were identified in Fig. 1h, corresponding to the {110} lattice planes of Cu_2O. The cubic shape and a single crystalline structure are confirmed by the results of XRD and TEM.

Based on the above observations, various uniformly sized Cu_2O nanocubes were obtained under different reaction conditions. The sizes and numbers of Cu_2O nanocubes obtained under the different reaction conditions were estimated from the total volumes and weights of the samples. The total volumes of Cu_2O nanocubes (*V*), calculated as weight/density (the density of Cu_2O is 6.0 g cm^{-3}), were 1.233×10^{-8} m^3, 1.283×10^{-8} m^3 and 1.281×10^{-8} m^3 in Samples A, B and C, respectively. The estimated numbers of Cu_2O nanocubes (*n*) were calculated using $n = VR^{-3}$ (where *V* is total volumes of Cu_2O nanocubes obtained in each sample and *R* denotes the length of an edge of the nanocube) as 8.523×10^{13}, 5.257×10^{13} and 2.753×10^{13} in samples A, B and C, respectively. However, the concentrations of free Cu ions in the initial reaction solution was estimated from the formation constant ($\log K_f = 7.2$)[15] of Cu–citrate and citrate concentration as 2.25, 1.50 and 0.75 mM in samples A, B and C, respectively, as presented in Table 1. The molar ratio of free Cu ion concentrations in A : B : C = 3 : 2 : 1, which is highly consistent with the ratio of the initial number of seeds in the solutions.

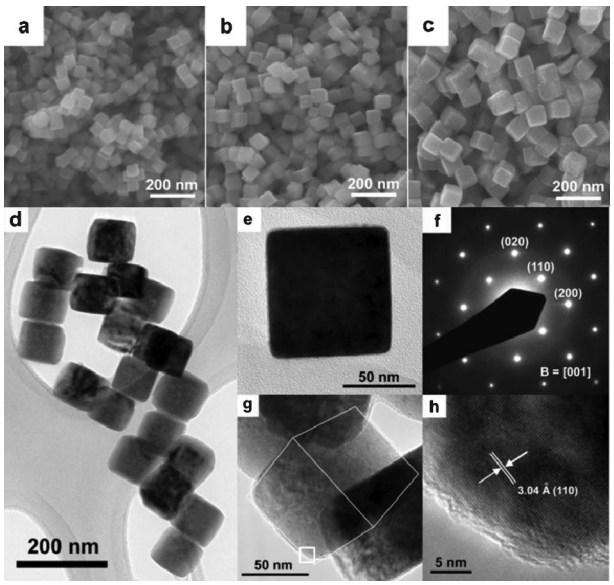

Fig. 1 SEM images of Cu_2O nanocubes samples. (a) Sample A; (b) sample B; (c) sample C. TEM images of Cu_2O nanocubes of sample C. (d) Low-magnification image; (e) high-magnification image; (f) SAED patterns of single Cu_2O nanocube; (g) image of tilted Cu_2O nanocube; (h) HR image of tilted nanocube.

The growth of Cu_2O nanocubes is described by the following equations.

$$Cu^{2+} + 2OH^- \rightarrow Cu(OH)_2 \quad (1)$$

$$2Cu(OH)_2 + C_6H_8O_6 \rightarrow Cu_2O + C_6H_6O_6 + 3H_2O \quad (2)$$

$$Cu^{2+} + \text{citrate}^{3-} \leftrightarrow Cu(\text{citrate})^- \quad (3)$$

The Scheme 1 presents a formation pathway for size-tunable Cu_2O nanocubes. In the absence of sodium citrate, Cu^{2+} ions precipitated out of basic solution as copper hydroxide very rapidly, as described by eqn (1). Then, the copper hydroxide was reduced by ascorbic acid to yield Cu_2O nanocubes, as described by eqn (2). However, if sodium citrate was added to the reaction solution prior to NaOH, the Cu^{2+} ions were chelated by citrate ions to form copper–citrate, preventing the precipitation of $Cu(OH)_2$ when NaOH was added, as in eqn (3). Varying the amount of sodium citrate altered the concentration of free Cu^{2+} ions in the growth solution (Scheme 1A), resulting in the formation of various amounts of $Cu(OH)_2$ precipitate in the basic solution, strongly affecting the initial step of growth. More sodium citrate in the reaction solution yielded fewer Cu^{2+} ions and Cu_2O particles at the beginning of the reaction. In the meanwhile, as Cu^{2+} ions were consumed, the equilibrium of eqn (3) moved to the left, releasing Cu^{2+} ions from the copper citrate and causing the ongoing growth and enlargement of the Cu_2O nanocubes. Accordingly, citrate chelating greatly reduced the initial concentration of the Cu_2O nanocube precursor, diminishing the nucleation of Cu_2O nanocubes, significantly increasing the size of the particles of Cu_2O nanocubes.

3d transition metal oxides (MO, where M is Fe, Co, Ni, Cu),[16,17] have been recognized as the potential anodes for Li-ion batteries. Cuprous oxide with theoretical capacity (375 mA h g^{-1}) has

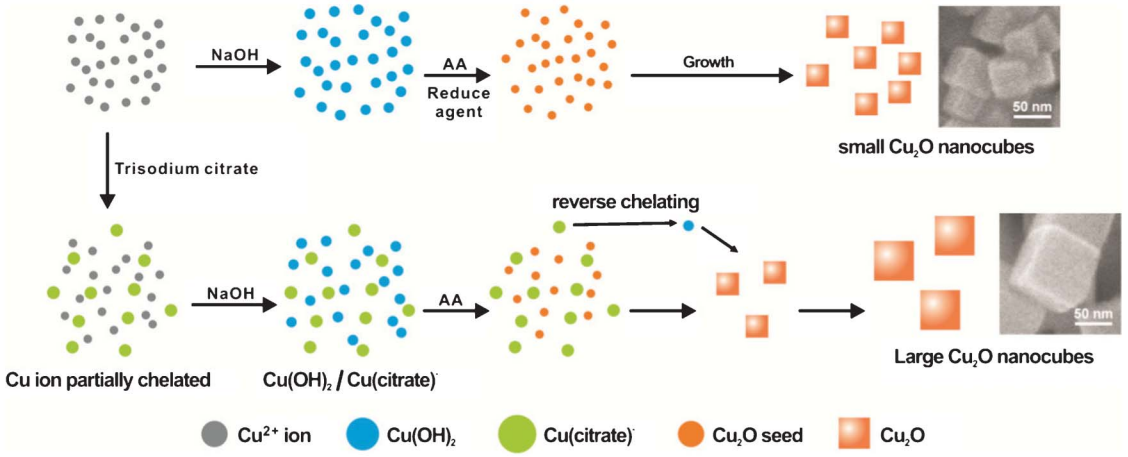

Scheme 1 Schematic illustration of the nanocube formation process *via* a nucleation-control growth approach.

attracted immense research attention and much progress has been made,[18,19] which is close to that of commercially used graphite (372 mA h g^{-1}). Fig. 2 shows cycling performance and Coulombic efficiency of Cu_2O electrodes (sample C) at a rate of 0.2 C and 1 C (1 C = 375 mA h g^{-1}). After 50 cycles, the discharge capacities of the electrodes (sample C) at a rate of 0.2 C and 1 C were 420 and 236 mA h g^{-1}, respectively. The electrode had a Coulombic efficiency of 96% after the first cycle. The superior battery performance was observed, as a result of small monodispersed Cu_2O nanocubes creating a large reactive site to the electrolyte. The formation and decomposition of SEI also contributes to the revealed capacities. The enhanced cycle behavior, makes Cu_2O nanocube a promising anode material for lithium-ion batteries (cyclic voltammetric curve, galvanostatic charge–discharge profiles and specific capability at various discharging and charging rates were shown in ESI,† S4 and S5).

In summary, a simple nucleation-controlled process for synthesizing a large amount of size-tunable Cu_2O nanocubes with a {100} side face was developed. The concentrations of sodium citrate significantly affect the size of Cu_2O nanocubes. In a reaction solution with a high concentration of citrate, Cu^{2+} ions preferentially formed copper citrate, disfavoring the fabrication of Cu_2O seeds, resulting in the growth of large Cu_2O nanocubes. The Cu_2O nanocubes anode performed excellently in a cyclic test at a rate of 0.2 C and 1 C, revealing the great potential of using Cu_2O nanocubes as an anode material in Li-ion batteries.

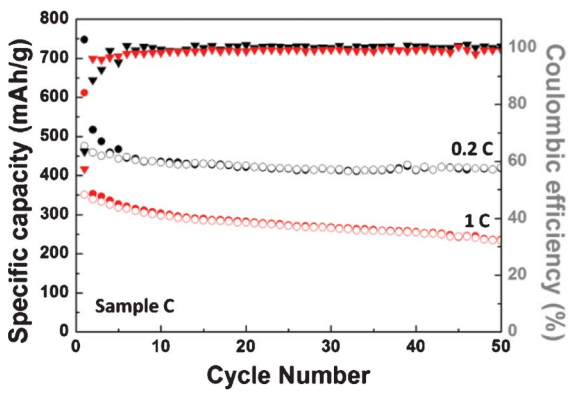

Fig. 2 Cycling performance of Cu_2O nanocube electrodes at a rate of 0.2 C and 1 C.

Acknowledgements

The authors like to thank the National Science Council of the Republic of China, Taiwan, for financially supporting this research under contract Nos. NSC 99-2113-M-007-011.

References

1 C. H. B. Ng and W. Y. Fan, *J. Phys. Chem. B*, 2006, **110**, 20801.
2 J. T. Zhang, J. F. Liu, Q. Peng, X. Wang and Y. D. Li, *Chem. Mater.*, 2006, **18**, 867.
3 H. Zhang, Q. Zhu, Y. Zhang, Y. Wang, L. Zhao and B. Yu, *Adv. Funct. Mater.*, 2007, **17**, 2766.
4 J.-H. Zhong, G.-R. Li, Z.-L. Wang, Y.-N. Ou and Y.-X. Tong, *Inorg. Chem.*, 2011, **50**, 757.
5 C.-H. Kuo, Y.-C. Yang, S. Gwo and M. H. Huang, *J. Am. Chem. Soc.*, 2011, **133**, 1052.
6 J. Y. Xiang, X. L. Wang, X. H. Xia, L. Zhang, Y. Zhou, S. J. Shi and J. P. Tu, *Electrochim. Acta*, 2010, **55**, 4921.
7 B. White, M. Yin, A. Hall, D. Le, S. Stolbov, T. Rahman, N. Turro and S. O'Brien, *Nano Lett.*, 2006, **6**, 2095.
8 M. Leng, M. Liu, Y. Zhang, Z. Wang, C. Yu, X. Yang, H. Zhang and C. Wang, *J. Am. Chem. Soc.*, 2010, **132**, 17084.
9 A. Paracchino, V. Laporte, K. Sivula, M. Graetzel and E. Thimsen, *Nat. Mater.*, 2011, **10**, 456.
10 C.-H. Kuo, C.-H. Chen and M. H. Huang, *Adv. Funct. Mater.*, 2007, **17**, 3773.
11 H. Xu, W. Wang and W. Zhu, *J. Phys. Chem. B*, 2006, **110**, 13829.
12 H. Xu and W. Wang, *Angew. Chem., Int. Ed.*, 2007, **46**, 1489.
13 L. Zhang and H. Wang, *ACS Nano*, 2011, **5**, 3257.
14 W. Z. Wang, G. H. Wang, X. S. Wang, Y. J. Zhan, Y. K. Liu and C. L. Zheng, *Adv. Mater.*, 2002, **14**, 67.
15 R. S. Juang and L. C. Lin, *Water Res.*, 2000, **34**, 43.

16 S. K. Behera, *Chem. Commun.*, 2011, **47**, 10371.
17 X. Wang, D.-M. Tang, H. Li, W. Yi, T. Zhai, Y. Bando and D. Golberg, *Chem. Commun.*, 2012, **48**, 4812.
18 P. Poizot, S. Laruelle, S. Grugeon, L. Dupont and J. M. Tarascon, *Nature*, 2000, **407**, 496.
19 S. Grugeon, S. Laruelle, R. Herrera-Urbina, L. Dupont, P. Poizot and J. M. Tarascon, *J. Electrochem. Soc.*, 2001, **148**, A285.

